Parameter Improved Particle Swarm Optimization Based Direct-Current Vector Control Strategy for Solar PV System

Pachaivannan NAMMALVAR[1], Subburam RAMKUMAR[2]
[1]*Department of Electrical and Electronics Engineering,*
Krishnasamy College of Engineering and Technology, Cuddalore, Tamil Nadu, India-607109.
[2]*Department of Electrical and Electronics Engineering,*
KPR Institute of Engineering and Technology, Coimbatore, Tamil Nadu, India-641407.
nammalvar@ifet.ac.in

***Abstract*—This paper projects Parameter Improved Particle Swarm Optimization (PIPSO) based direct current vector control technology for the integration of photovoltaic array in an AC micro-grid to enhance the system performance and stability. A photovoltaic system incorporated with AC micro-grid is taken as the pursuit of research study. The test system features two power converters namely, PV side converter which consists of DC-DC boost converter with Perturbation and Observe (P&O) MPPT control to reap most extreme power from the PV array, and grid side converter which consists of Grid Side-Voltage Source Converter (GS-VSC) with proposed direct current vector control strategy. The gain of the proposed controller is chosen from a set of three values obtained using apriori test and tuned through the PIPSO algorithm so that the Integral of Time multiplied Absolute Error (ITAE) between the actual and the desired DC link capacitor voltage reaches a minimum and allows the system to extract maximum power from PV system, whereas the existing d-q control strategy is found to perform slowly to control the DC link voltage under varying solar insolation and load fluctuations. From simulation results, it is evident that the proposed optimal control technique provides robust control and improved efficiency.**

***Index Terms*—solar energy, particle swarm optimization, optimal control, power conditioning, microgrids.**

I. INTRODUCTION

Since fossil fuel power generation system has major disadvantages and environmental pollution, renewable energy sources is an admirable alternative solution for fossil fuel exhaustion. Nowadays, renewable power sources such as solar cells, hydrogen-fuel cells and wind energy conversion systems are used in power electronics interface [1] as essential elements for grid integration.

During the availability of sunlight, boost DC/DC converter and the Grid-Side Voltage Source Converter (GS-VSC) can transform solar energy to local load and utility grid. However, in the absence of sunlight, the power required for local loads is consumed directly from the main AC grid. Since GS-VSC has been located widely at the feeder tail end, reactive power compensation becomes more operative for load-side consumer voltage support. In grid-connected condition, the commercial inverters mainly inject active power only to the grid [2-3].

On the other hand, it is possible to integrate power quality functions by compensating the reactive power of the local loads. The reactive power capacity of the voltage source inverter is limited by the current-carrying capability of the Insulated Gate Bipolar Transistor (IGBT) and dc-link voltage. In the meantime, solar photo voltaic output power is at all times less than the inverter rated power and its remaining capacity can be used for the reactive power supply [4-5].

The reactive power, voltage control and harmonics current compensation methods are conferred for distribution generation systems in [6-7]. The grid connected power quality compensator with distribution generation can control not only the active power flow, but also can alleviate load unbalance, harmonics, and manage reactive power by using Instantaneous Reactive Power (IRP) theory and the Synchronous Reference Frame (SRF) theory. These theories are mostly addressed in the literature [8].

The performance of a GS-VSC in AC micro-grid depends not just on type of converter topologies but also on how the converter has been controlled. Conventionally, controlling of a GS-VSC in AC micro-grid as well as the converter in STATCOM employs the traditional decoupled d-q vector control scheme [9-10]. The performance of the controller has not been discussed in detail, when the converter works below and above the linear modulation limit [11-12]. The origin of this work shows that there are some limitations in the d-q vector control strategy, and the output seems to be large oscillations in the GS-VSC grid connected systems, specifically when the converter works above its linear modulation margin. This paper proposes an optimal PIPSO based tuning for the PI controllers in the direct current vector control approach for a GS-VSC. The purpose of the proposed control technique is to maintain a constant dc capacitor voltage in order to improve the system efficiency and to enhance the system stability both within and beyond the converter linear modulation limit. It compared with the results obtained from the conventional tuning of the PI controller.

The rest of the paper has been organized as follows: the configuration and different operating modes of a test system are focused in Section 2. Section 3 proposes an optimal control philosophy. Section 4 presents simulation study and the system performance comparison. Finally, the Section 5 is concluded with the summary of the main points.

Digital Object Identifier 10.4316/AECE.2018.01013

II. System Configuration and Operation

A. AC Micro-Grid and Circuit Configuration

The layout diagram of the AC micro-grid is shown in Fig.1. PV side DC/DC boost converter operates using Perturb and Observe (P&O) based Maximum Power Point Tracking (MPPT) technique [13-14] whereas grid side inverter GS-VSC employs the proposed PIPSO based optimal direct current vector control.

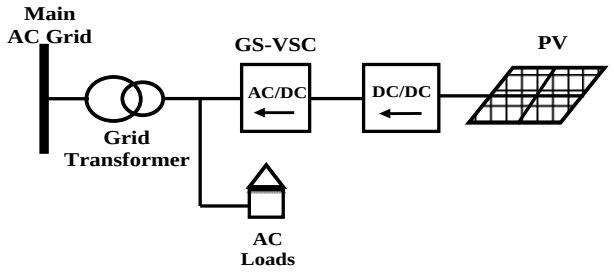

Figure 1. Layout of AC micro-grid for integration of PV

B. Operating Modes

The primary objective of this proposed work is to extract maximum amount of energy from the PV module and that improves the system stability and efficiency with the assistance of optimal control technique. Power flow model of the proposed AC micro-network is classified into three different operating modes.

Mode-I: When there is no AC local load demand at the Point of Common Coupling (PCC), whatever the electric power generated by PV module is completely fed into the main AC grid.

Mode-II: While the power produced from PV source is greater than the demanded power of local loads, the remaining surplus energy of PV is exported to the main grid.

Mode-III: During sunset or dimness of sunlight, the intensity of solar energy falling on PV module is insufficient. In this situation, to meet out the local AC loads, the system imports the remaining required power from the main AC grid.

III. GS-VSC Control Method

Fig. 3 depicts the proposed PIPSO based direct-current vector control strategy of GS-VSC. It has a nested loop topology which comprises an outer slow voltage loop and an inner fast current loop that produce d-axis and q-axis current references (i^*_d and i^*_q) [15]. The function of inner current controller is to minimize the two current errors such as the d-axis current error between the d-axis current reference i^*_d and the actual d-axis current component; and the q-axis current error between the q-axis current reference i^*_q and the actual q-axis current component. The outer voltage controller consists of a DC link voltage control and AC bus voltage or reactive power control. The DC voltage control can alter the d-axis current reference $i^*_{d,}$ according to the difference between the actual and the reference capacitor voltages, whereas AC voltage control alters the q-axis current reference i^*_q depending on the difference between the actual and the reference AC bus voltages. The main function of DC link voltage control employed in the d-q vector control is to control the active power flow between the AC bus and the DC link of VSC.

The equations (1) and (2) are arrived from the reference frame voltage balance equation of the AC system. The three phase sinusoidal converter output voltage depends on the d-axis and the q-axis references of v^*_{a1}, v^*_{b1} and v^*_{c1} are produced from the two voltage references v^*_{d1} and v^*_{q1} to control the VSC. The d and q axis components of grid voltage v_d & v_q, and v'_d & v'_q are transferred from the current controllers and whereas the low pass inductor filter mentioned as L, ω_s is the angular frequency of the grid voltage.

$$v^*_{d1} = -v'_d + \omega_s L i'_q + v_d \quad (1)$$

$$v^*_{q1} = -v'_q - \omega_s L i'_d \quad (2)$$

The voltage control signals v'_d and v'_q from the outer controller are used to regulate the current control signals i_d and $i_{q,}$ respectively. From the view point of d-q vector control technique, it can be well understood that the real power control is more efficiently regulated by q-axis voltage whereas the reactive power control is more efficiently regulated by d-axis voltage. Hence, the standard vector control technique depends especially on compensation elements rather than the PI controllers to control the d-axis and q-axis current components. In order to utilize the advantage of optimal PI control logic, the d-q vector control method is modified to improve the system efficiency and performance and an optimal PIPSO based direct-current vector control is proposed in the next section. The proposed control system uses d-axis current for active power control and q-axis current for grid voltage support control.

A. PIPSO Based Optimal Direct-Current Vector Control for GS-VSC

In this section, a novel PIPSO based approach is presented in designing the PI controller gain variables for the proposed direct-current vector controlled system [16-18]. The parameters of proportional and integral gain control variables (K_p) and (K_i) of PI controller are being optimized using PIPSO algorithm. The fitness function has been developed by considering the system parameters such as rise time, peak over-shoot, settling time and steady state error to optimize the parameter of the PI controller. Normally, the performance indices such as Integral of Squared Error (ISE), Integral of Time multiplied Squared Error (ITSE), Integral of Time Multiplied by Absolute Error (ITAE) and Integral of Absolute Error (IAE) are applied for the optimization of controller. Based on the investigations, it is found that ITAE offers good system stability with reduced oscillations and also minimizes the fitness function [19]. ITAE for the optimal design of PI controller is given by the equation (3)

$$ITAE = \int t \left| V^*_{dc} - V_{dc} \right| dt \quad (3)$$

Where, V^*_{dc} and V_{dc} are the desired and the actual DC-link capacitor voltages, respectively and 't' is the simulation step time.

In general, the d-q vector control has four PI controllers, two at inner current loop and the remaining at outer voltage loop. In the proposed study, the gain of the PI controllers at outer voltage loop (AC voltage control and DC voltage control) is kept constant and the optimal tuning of PI controller gains by PIPSO is implemented at the inner current loop. The values of the proportional (K_p) and the

integral (K_i) controller gains of outer voltage loop controllers are shown in the Table I. Table II shows the PI controller gain at inner current loop of upper and lower limits obtained by PIPSO optimal tuning for each controller.

TABLE I. CONTROLLER GAINS FOR OUTER VOLTAGE LOOP

Parameters	Proportional Gain (K_p)	Integral Gain (K_i)
AC Voltage regulation	0.55	2500
DC Voltage regulation	0.001	0.15

TABLE II. RANGE OF PI CONTROLLER GAINS FOR OPTIMAL TUNING – CURRENT LOOP

Parameters	Proportional Gain (K_p)		Integral Gain (K_i)	
	min	max	min	max
d-axis	0.643	0.958	160	240
q-axis	0.625	0.942	158	238

B. Parameter Improved Particle Swarm Optimization Algorithm (PIPSO)

The concept of PSO algorithm to solve the optimization problems was discovered by Eberhart and Kennedy in 1995 [20]. PSO technique has been developed from the natural behavior of birds flocking or fish schooling. By extending the concept of existing particle swarm optimization algorithm, PIPSO based technique has been developed. The basic PSO algorithm explores the global optimum solution from a given search space. The position and velocity of the i^{th} particle of the swarm in the D-dimensional vector are represented as $x_i=[x_{i1},x_{i2},...,x_{iD}]$ and $v_i=[v_{i1},v_{i2},...,v_{iD}]$, respectively. The local and the global best position are represented as $p_i=[p_{i1},p_{i2},...,p_{iD}]$ and $p_g=[p_{g1},p_{g2},...,p_{gD}]$, respectively. The position and velocity of each particle are updated in the next iterations by using the following equations.

$$v_i^{n+1} = \omega\, v_i^n + \varphi_1 (p_i^n - x_i^n) + \varphi_2 (p_g^n - x_i^n) \quad (4)$$

$$x_i^{n+1} = x_i^n + v_i^{n+1} \quad (5)$$

Where, *(i = 1,2,..., m)*, n is the iteration number, ω is the inertia weight, $\varphi_1=c_1r_1$ and $\varphi_2=c_2r_2$, c_1 and c_2 are two positive acceleration coefficients called social and cognitive agents, respectively. Both r_1 and r_2 are random numbers uniformly distributed in between 0 to 1.

The parameters of the PIPSO such as ω, c_1 and c_2 are improved by the following equations,

$$\omega_1 = \omega_{\max} - \frac{\omega_{\max} - \omega_{\min}}{n_{\max}} \times n \quad (6)$$

$$\omega = \omega_{\min} + \omega_1 \times r_3 \quad (7)$$

$$c_1 = c_{1\max} - \frac{c_{1\max} - c_{1\min}}{n_{\max}} \times n \quad (8)$$

$$c_2 = c_{2\max} - \frac{c_{2\max} - c_{2\min}}{n_{\max}} \times n \quad (9)$$

Where, ω_{min} and ω_{max} are the minimum and the maximum weights, c_{1min} and c_{1max} are the minimum and the maximum cognitive factors, c_{2min} and c_{2max} are the minimum and the final social factors, n_{max} is the maximum iteration and r_3 is random numbers uniformly distributed in between 0 and 1.

C. Implementation

Let '*m*' is the number of populations and '*n*' is the number of iterations. The flowchart of the PIPSO algorithm is shown in Fig. 2. The step by step procedures of the implementation of proposed method to find optimal controller gain parameters are as follows,

Step 1: Read PIPSO parameters such as *m, n,* n_{max}, (ω_{min} and ω_{max}), (c_{1min} *and* c_{1max}) and (c_{2min} *and* c_{2max}).

Step 2: Set initial iteration number as $n = 1$.

Step 3: Arbitrarily assign initial working solutions for 'm' particles in vector form as $x_i=[x_{i1}\ x_{i2}]$, *i = 1 to m*; where x_{i1} represents proportional gain and x_{i2} represents integral gain of the Proportional-Integral (PI) controller.

Step 4: For each particle i, calculate fitness function ITAE of the test system using (3) to i^{th} particle. Repeat this step for all other particles.

Step 5: Find out the i^{th} particle's local best position p_i and velocity v_i.

Step 6: Modify the swarm weight factors using equations (6) - (9).

Step 7: For each particle i, carry out velocity update using (4) and qualify their positions using (5).

Step 8: Calculate the global best position p_g among the best particle.

Step 9: Examine whether the selected best swarm positions meet the problem requirements. If any position vector dissatisfies, then initialize new solutions for the violated swarm as stated in step 3; otherwise, proceed to the following step 10.

Step 10: If the convergence criteria are satisfied (*n* equals n_{max}), output the optimal gains of the controllers; otherwise set $n = n + 1$, and repeat the steps 4 to 10.

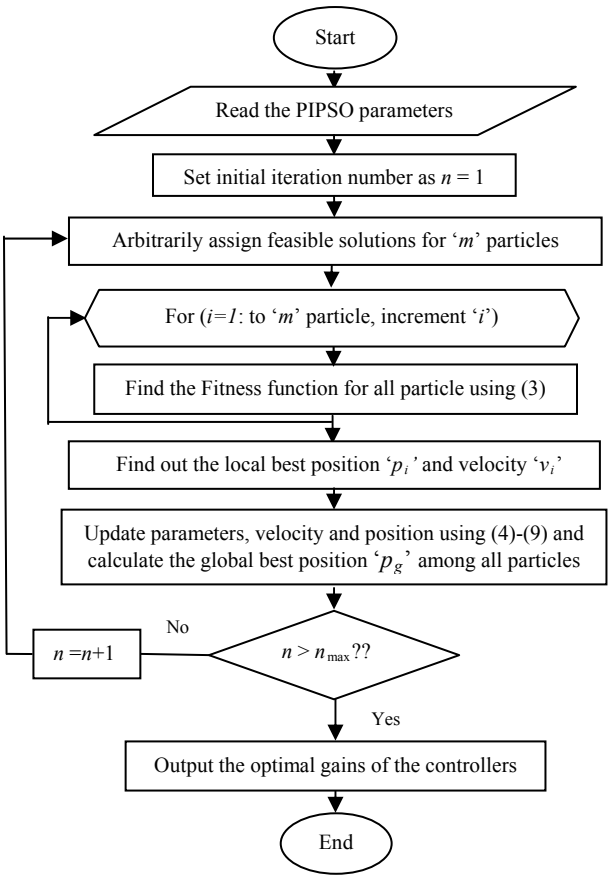

Figure 2. Flowchart of the PIPSO algorithm

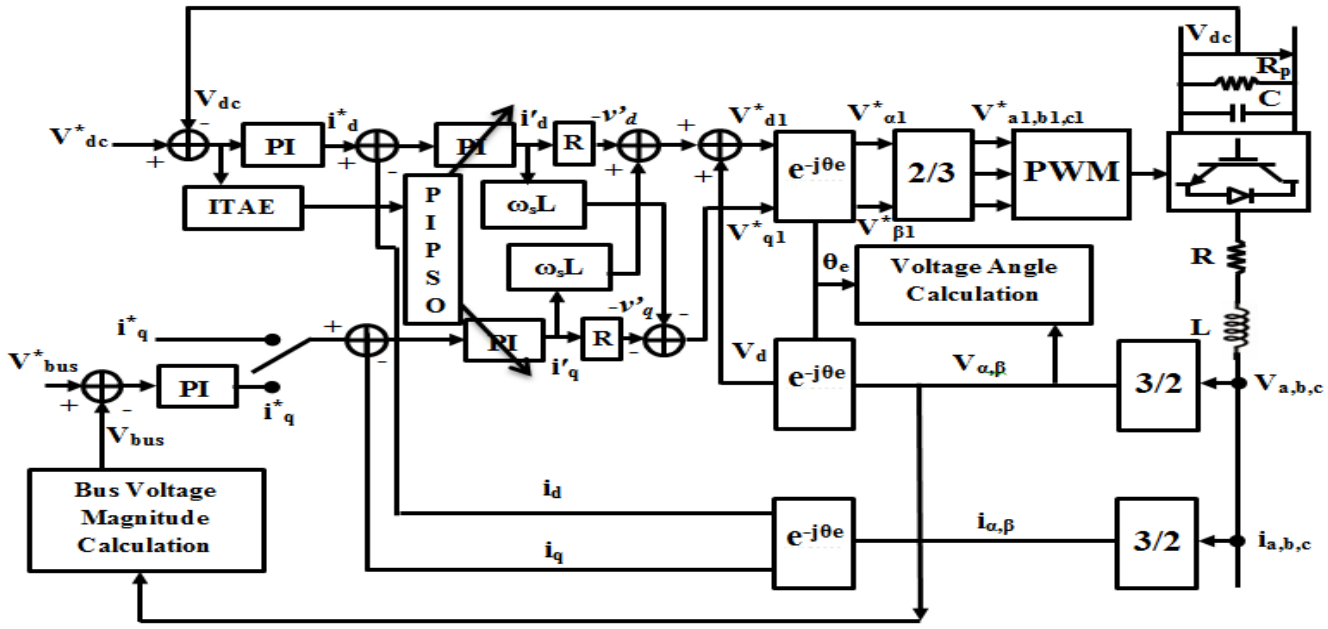

Figure 3. Proposed PIPSO based direct current vector control scheme for GS-VSC

IV. Case Studies and Simulation Results

In order to examine the prevalence and quality of the proposed control scheme, a MATLAB/Simulink model has been developed for an AC test system. The modeled test system with standard d-q vector control and the proposed optimum control is simulated separately for three different operating environments. The performance has been examined with three case studies over the period of operation. Though the process may be continuous still the best values of the gains obtained from the three cases has been used with a presumption that it will allow the PIPSO for assuring at the desired performance. The inferences obtained from the simulation studies are used to observe the performance efficiency and superiority of the DC-DC converter and GS-VSC in terms of maximizing the power extract from the PV panel, controlling the DC capacitor voltage and delivering maximum possible renewable energy to an AC micro grid. During the time domain analyzation, the effect of solar insolation variation is considered. At first, the solar insolation is maintained at 1000 W/m^2 for 1 sec, and then, the solar insolation is varied randomly between 800 W/m^2 to 1000 W/m^2 for every 1 second. The entire simulation is carried out for a period of 10 seconds and the average value of solar insolation falling on the PV panel is assumed as 910 W/m^2. The following section details three simulation case studies. In all the case studies, the effectiveness of the proposed PIPSO based control scheme is compared with the d-q control scheme.

A. Case-1

In this case study, the renewable PV source is interconnected with an AC micro grid through DC-DC converter and GS-VSC and also it is assumed that there is no live AC load present nearer to the Point of Common Coupling (PCC). During the time domain analyzation, the PV side DC-DC converter is about to operate under MPPT mode in order to achieve maximum power extracts from the solar panel and the GS-VSC is committed to control the DC capacitor terminal voltage. The power exported to AC micro grid and the DC power extracted from the PV panel with respect to the effect of sun light intensity variation are studied and the corresponding simulation responses are depicted in Fig. 4(a) – (c). Figs. 5(a) – (c) show the voltage response of the DC capacitor and PV terminal for different solar insolation levels. It can be concluded that the GS-VSC with proposed PIPSO based direct current vector control strategy can smoothly regulate the DC-link voltage, during solar insolation variation.

B. Case-2

The generated PV power integrated with an external AC micro-grid along with fixed 50kW local AC load is considered in this analysis. During the simulation, the PV is operated under MPPT mode, and the GS-VSC regulates the DC voltage. The effect of solar insolation variation is considered in the simulation and it is shown in Fig. 6(a). The Power exported to AC micro-grid, Local AC load power and PV power are illustrated in Figs. 6(b) - (d), respectively. DC voltages at the DC-link of VSC are shown in Fig. 7(b). Fig. 7(c) also shows the PV array MPP voltage for different solar insolation levels. It is inferred that the GS-VSC with proposed PIPSO based direct current vector control strategy can efficiently control the DC-link voltage during solar insolation variation.

C. Case-3

In this test case, the PV generation system is compared with the conventional and the proposed control strategies under situations like cloudy days. In this situation, the intensity of solar radiation falling over PV panel will be low and also the electric power extraction is very minimum. To meet out the reliable operation of local AC loads at PCC, the system imports the remaining required power from the main AC grid. During the simulation, the PV is operated under MPPT mode and the GS-VSC regulates the DC voltage. Similar to previous case studies, the effects of both solar insolation variation and load variation are considered for the

validation. Power exported/imported to AC micro-grid, AC load power and PV power are illustrated in Figs. 8(b) - (d), respectively. DC voltages at the DC-link of VSC are shown in Fig. 9(b). Fig. 9(c) also shows the PV array MPP voltage for different solar insolation levels. It is seen that the GS-VSC with the proposed controller can proficiently maintain the DC capacitor voltage during solar insolation variation and the terminal voltage of GS-VSC is also regulated under different loading conditions.

Table III illustrates the details of power export, import and local load utilization during the simulation sample time period of 0 to 1 seconds for the solar insolation value at 1000 W/m^2.

TABLE III. DIFFERENT OPERATING SCENARIOS

Modes	Solar Power (P_{pv})	Power Exported to Grid (P_{grid})	Power Imported from Grid (P_{grid})	Local AC Loads (P_{Load})
Case-1	100 kW	100 kW	0 kW	0 kW
Case-2	100 kW	50 kW	0 kW	50 kW
Case-3	50 kW	0 kW	50 kW	100 kW

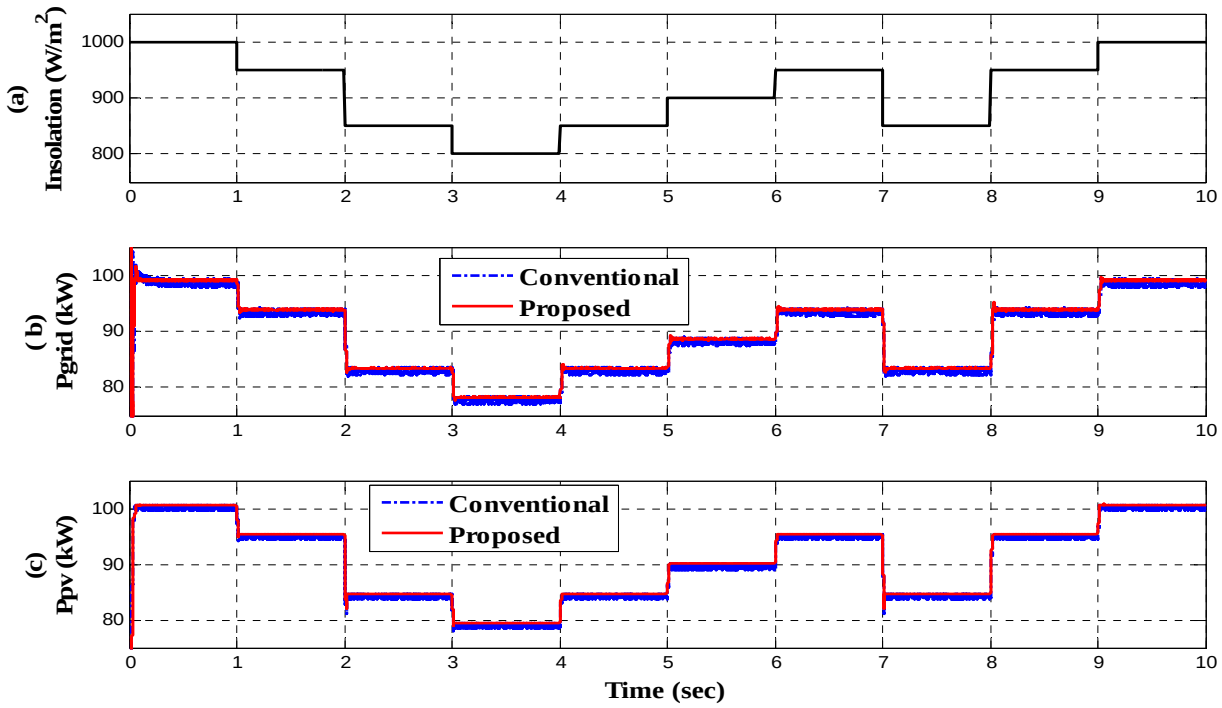

Figure 4. System operation during PV generation variation in grid connected mode (Case-1), (a) Solar insolation variation (W/m^2), (b) Total power exported to grid (kW), (c) PV power generation (kW).

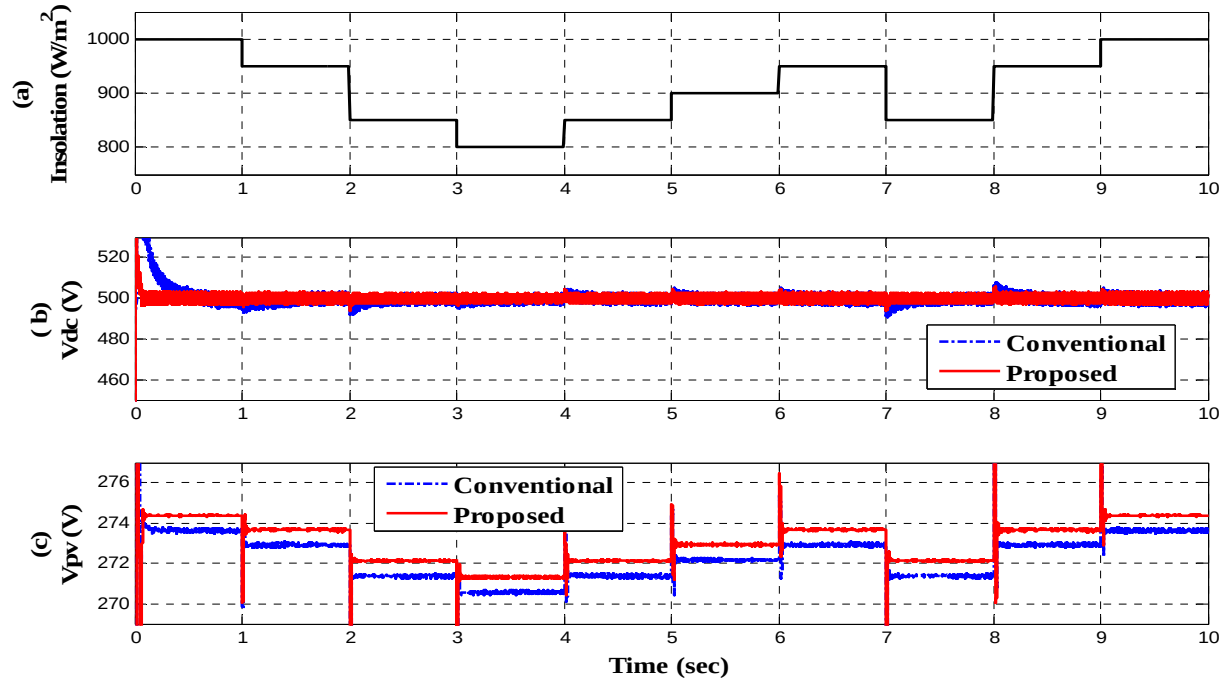

Figure 5. System operation during PV generation variation in grid connected mode (Case-1), (a) Solar insolation variation (W/m^2), (b) DC-link voltage at GS-VSC (V), (c) PV array voltage (Volts).

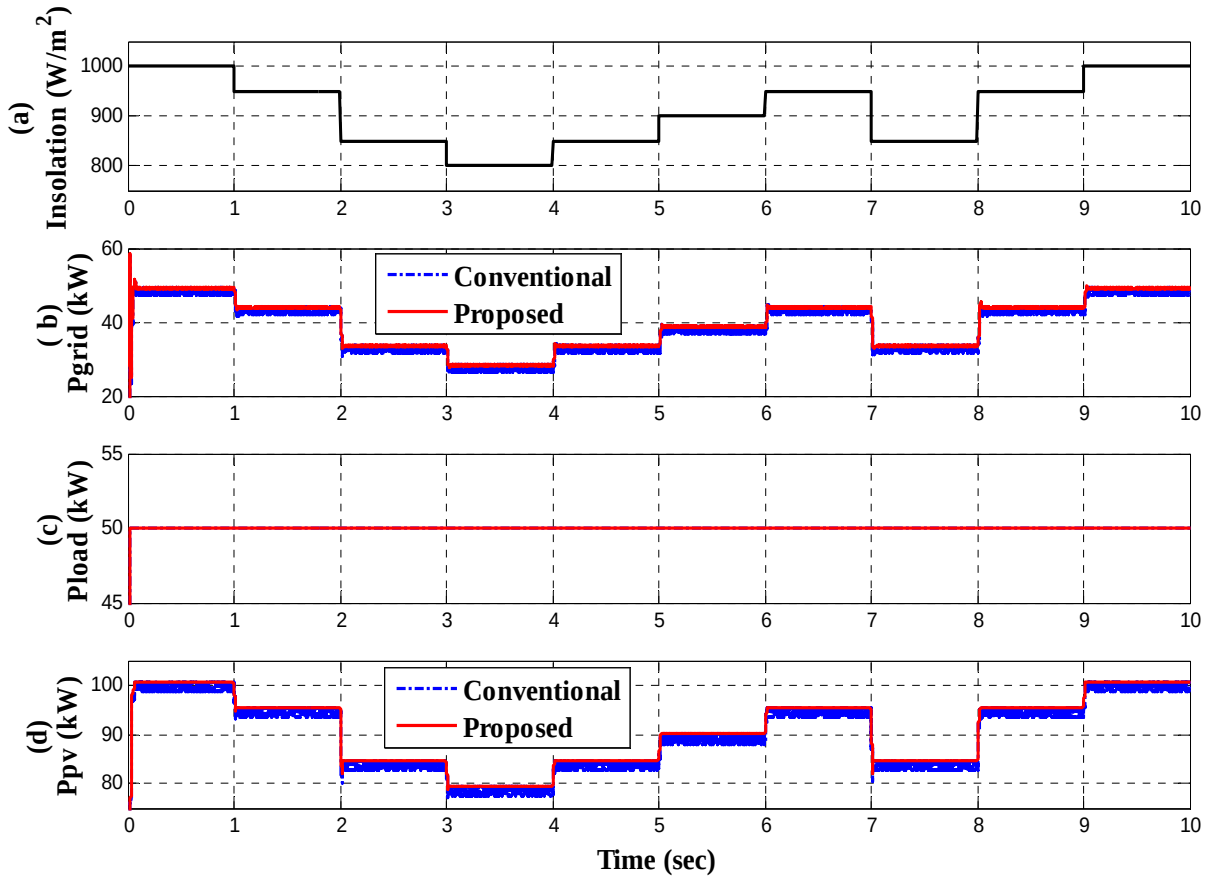

Figure 6. System operation during PV generation variation in grid connected mode with fixed 50kW local AC load (Case-2), (a) Solar insolation variation (W/m^2), (b) Total power exported to grid (kW), (c) Total power consumed by local AC load (kW), (d) PV power generation (kW).

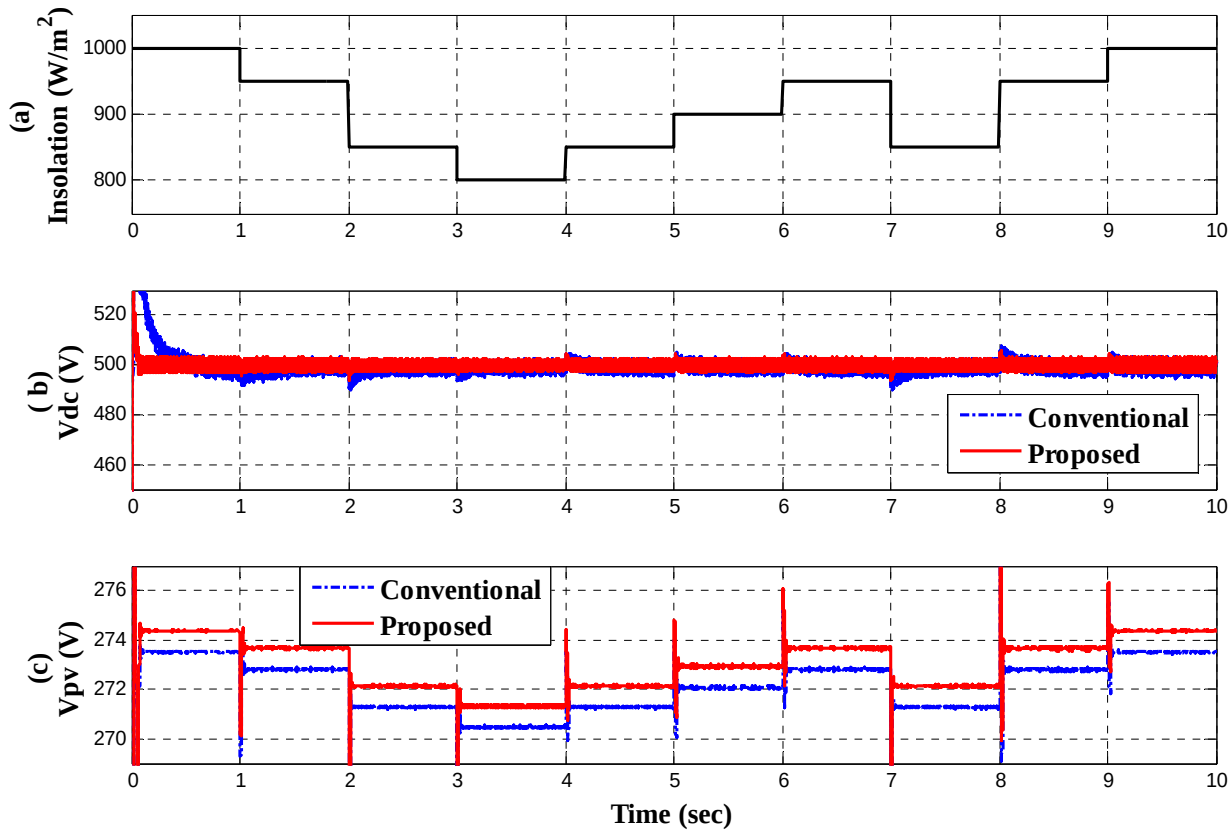

Figure 7. System operation during PV generation variation in grid connected mode with fixed 50kW local AC load (Case-2), (a) Solar insolation variation (W/m^2), (b) DC-link voltage at GS-VSC (V), (c) PV array voltage (Volts).

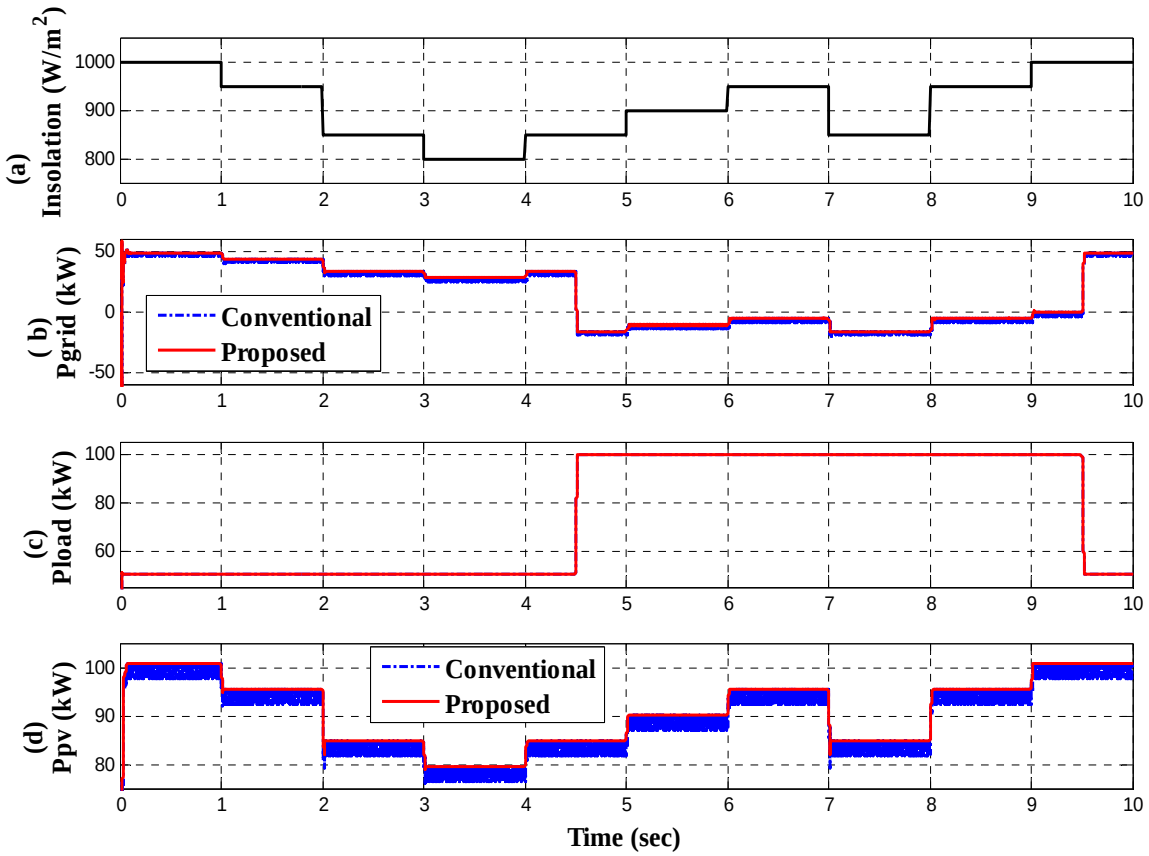

Figure 8. System operation during PV generation variation in grid connected mode with variable local AC load (Case-3), (a) Solar insolation variation (W/m^2), (b) Total power exported/imported to grid (kW), (c) Total power consumed by variable local AC load (kW), (d) PV power generation (kW).

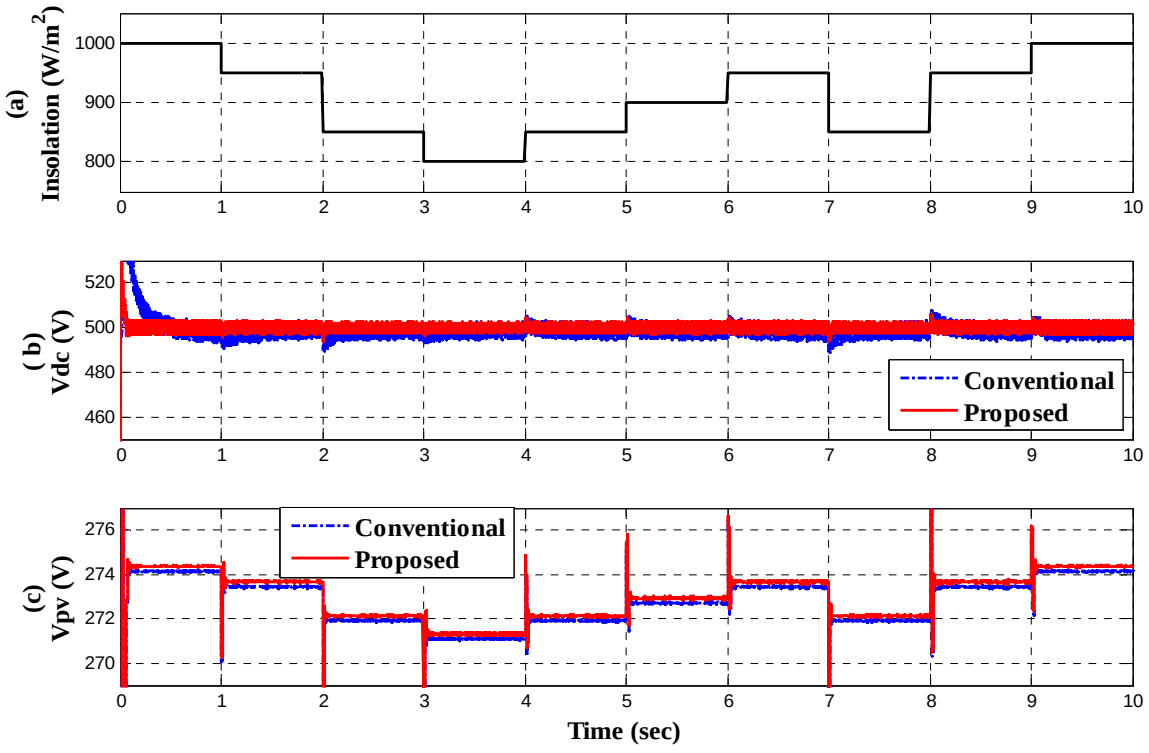

Figure 9. System operation during PV generation variation in grid connected mode with variable local AC load (Case-3), (a) Solar insolation variation (W/m^2), (b) DC-link voltage at GS-VSC (V), (c) PV array voltage (Volts).

The comparisons of power conversion efficiency of the existing control method and the proposed optimal PIPSO based direct-current vector control strategy for different case studies are reported in the Table IV. From the Table IV, it is

evident that the proposed optimal direct current vector control scheme has better performance than the existing control scheme. Even for time varying solar insolation and different loading conditions, the power extraction efficiencies of both the DC-DC converter and GS-VSC outperform compared to the d-q controller. For all the simulation cases carried out in this study, the power conversion efficiency is improved than that of d-q vector control method. The Table IV shows that the proposed optimal direct current vector control scheme not only just possesses good stability and efficiency but also it shows solid performance against time varying solar insolation under different loading conditions.

TABLE IV. COMPARISON OF POWER CONVERSION EFFICIENCY OF EXISTING AND PROPOSED CONTROL STRATEGY FOR VARIOUS CASES

Technique	Case-1		Case-2		Case-3	
	d-q Vector Control	PIPSO based Direct Current Vector Control	d-q Vector Control	PIPSO based Direct Current Vector Control	d-q Vector Control	PIPSO based Direct Current Vector Control
Average Solar insolation (W/m^2)	910	910	910	910	910	910
Average Power extracted from PV panel (kW)	90.38	90.86	89.86	90.86	89.36	90.86
Average Power exported to gird (kW)	88.95	89.44	88.55	89.56	87.93	89.43
Power conversion efficiency at DC-DC converter (%)	99.31	99.84	98.74	99.84	98.19	99.84
Power conversion efficiency at GS-VSC (%)	97.74	98.28	97.30	98.41	96.62	98.27

V. CONCLUSION

This paper purports PIPSO based optimal direct current vector control technique for GS-VSC in a photovoltaic incorporated AC micro-grid under load fluctuations and solar insolation variation. The maintenance of constant voltage at DC link capacitor and at GS-VSC is recognized as the objective of the proposed control scheme by conceiving two different operating modes such as power exported to the main utility grid and power imported from the grid. The aggregations of the proposed control strategy and MPPT technique enable maximum utilization of power extract from the PV modules, during time varying solar insolation and load perturbation. The simulation studies have been implemented in MATLAB Simulink environment and it is verified that the proposed control scheme has improved system stability and power conversion efficiency over the d-q vector control in renewable energy source integrated AC micro-grid.

REFERENCES

[1] F. Blaabjerg, Z. Chen, S. B. Kjaer, "Power electronics as efficient interface in dispersed power generation systems," IEEE Trans. Power Electron, vol. 19, no. 5, pp. 1184-1194, 2004, doi:10.1109/TPEL.2004.833453

[2] Y. Yang, F. Blaabjerg, H. Wang, M.G. Simoes, "Power control flexibilities for grid-connected multi-functional photovoltaic inverters," IET Renewable Power Generation, vol.10, no.4, pp.504-513, 2016, doi:10.1049/iet-rpg.2015.0133

[3] M. Unlu, S. Camur, E. Beser, B. Arifoglu, "A Current-Forced Line-Commutated Inverter for Single-Phase Grid-Connected Photovoltaic Generation Systems," Advances in Electrical and Computer Engineering, vol.15, no.2, pp.85-92, 2015, doi:10.4316/AECE.2015.02011

[4] D. Yazdani, A. Bakhshai, G. Joos, M. Mojiri, "A real-time extraction of harmonic and reactive current in a nonlinear load for grid-connected converters," IEEE Transactions on Industrial Electronics, vol.56, no.6, pp.2185-2189, 2009, doi:10.1109/TIE.2009.2017100

[5] M. Asit, M. Viswavandya, M. Sthitapragyan, K. Prakash, S. Patra, "Modelling, simulation and optimisation of robust PV based micro grid for mitigation of reactive power and voltage instability," International Journal of Electrical Power & Energy Systems, vol.81, pp.444-458, 2016, doi:10.1016/j.ijepes.2016.02.027

[6] Y. A. Hajizadeh, M. A. Golkar, A. Feliachi, "Voltage control and active power management of hybrid fuel-cell/energy-storage power conversion system under unbalanced voltage sag conditions," IEEE Transactions on Energy Converters, vol. 25, no.4, pp.1195-1208, 2010, doi:10.1109/TEC.2010.2062516

[7] A. Cagnano, E. Tuglie, M. De Liserre, R. A. Mastromauro, "Online optimal reactive power control strategy of PV inverters," IEEE Transactions on industrial Electronics, vol.58, no.10, pp.4549-4558, 2011, doi:10.1109/TIE.2011.2116757

[8] E. Sundaram, M. Venugopal, "On design and implementation of three phase three level shunt active power filter for harmonic reduction using synchronous reference frame theory," International Journal of Electrical Power & Energy Systems, vol.81, pp.40-47, 2016, doi:10.1016/j.ijepes.2016.02.008

[9] T. Zaveri, B. Bhalja, N. Zaveri, "Comparison of control strategies for DSTATCOM in three-phase, four-wire distribution system for power quality improvement under various source voltage and load conditions," International Journal of Electric Power Energy System, vol.43, pp.582-594, 2012, doi:10.1016/j.ijepes.2012.06.044

[10] D. Kairus, R. Wamkeue, B. Belmadani, M. Benghanem, "Variable Structure Control of DFIG for Wind Power Generation and Harmonic Current Mitigation," Advances in Electrical and Computer Engineering, vol.10, no.4, pp.167-174, 2010, doi:10.4316/AECE.2010.04027

[11] S. Li, L. Xu, T. A. Haskew, "Control of VSC-based STATCOM using conventional and direct-current vector control strategies," International Journal of Electrical Power & Energy Systems, vol.45, no.1, pp.175-186, 2013, doi:10.1016/j.ijepes.2012.08.060

[12] S. Li, I. Jaithwa, R. Suftah, X. Fu, "Direct-current Vector Control of Three-phase Grid-connected Converter with L, LC, and LCL Filters," Electric Power Components and Systems, vol.43, no.14, pp.1644-1655, 2015. doi:10.1080/15325008.2015.1045310

[13] A. L. Alhamdawee, N. F. Mailah, M. A. Radzi, S. B. Shafie, S. Hajighorbani, A. Q. Turki, "Comparison of developed FLC and P&O MPPT algorithms for improving PV system performance at variable irradiance conditions," World Journal of Engineering, vol. 13, no. 6, pp.494-499, 2016, doi:10.1108/WJE-09-2016-0082

[14] A. Durusu, I. Nakir, A. Ajder, R. Ayaz, H. Akca, M. Tanrioven, "Performance Comparison of Widely-Used Maximum Power Point Tracker Algorithms under Real Environmental Conditions," Advances in Electrical and Computer Engineering, vol.14, no.3, pp.89-94, 2014, doi:10.4316/AECE.2014.03011

[15] F. Liu, Y. Zhou, S. Duan, J. Yin, B. Liu, F. Liu, "Parameter Design of a Two-Current-Loop Controller Used in a Grid-Connected Inverter System with LCL Filter," IEEE Transactions on Industrial Electronics, vol.56, no.11, pp.4483-4491, 2009, doi:10.1109/TIE.2009.2021175

[16] M. Gecic, M. Kapetina, D. Marcetic, "Energy Efficient Control of High Speed IPMSM Drives - A Generalized PSO Approach," Advances in Electrical and Computer Engineering, vol.16, no.1, pp.27-34, 2016, doi:10.4316/AECE.2016.01004

[17] G. Chen, L. Liu, Y. Gua, S. Huang, "Multi-objective enhanced PSO algorithm for optimizing power losses and voltage deviation in power systems," COMPEL: The International Journal for Computation and Mathematics in Electrical and Electronic Engineering, vol. 35, no.1, pp.350-372, 2016, doi:10.1108/COMPEL-02-2015-0030

[18] K. Dezelak, P. Bracinik, M. Hoger, A. Otcenasova, "Comparison between the particle swarm optimisation and differential evolution approaches for the optimal proportional–integral controllers design during photovoltaic power plants modelling," IET Renewable Power Generation, vol.10, no.4, pp.522-530, 2016, doi:10.1049/iet-rpg.2015.0108

[19] F. Padula, A. Visioli, "Tuning rules for optimal PID and fractional-order PID controllers," Journal of process control, vol.21, no.1, pp.69-81, 2011, doi:10.1016/j.jprocont.2010.10.006

[20] R. Eberhart, J. Kennedy, "A new optimizer using particle swarm theory," Sixth Symposium on Micro Machine and Human Science, IEEE Service Center, Piscataway, pp.39-43, 1995, doi:10.1109/MHS.1995.494215